Available online at BCREC website: https://bcrec.id

Bulletin of Chemical Reaction Engineering & Catalysis, 17 (3) 2022, 486-496

Research Article

Enhancement in Photocatalytic Efficiency of Commercial TiO_2 Nanoparticles by Calcination: A Case of Doxycycline Removal

Nguyen Thi Cam Tien, Chau Hong Nhut, Vo Thi Thanh Thuy, Trinh Thi Bich Huyen, Lam Pham Thanh Hien, Nguyen Nhat Huy*

[1]*Faculty of Environment and Natural Resources, Ho Chi Minh City University of Technology (HCMUT), 268 Ly Thuong Kiet St., Dist. 10, Ho Chi Minh City, Vietnam.*
[2]*Vietnam National University Ho Chi Minh City, Linh Trung Ward, Thu Duc City, Ho Chi Minh City, Vietnam.*

Received: 29th March 2022; Revised: 17th June 2022; Accepted: 20th June 2022
Available online: 22nd June 2022; Published regularly: September 2022

Abstract

In this study, the pure and calcined forms of Degussa TiO_2 were applied for photocatalytic removal of doxycycline - a broad-spectrum tetracycline antibiotic. The calcination of TiO_2 at 500 °C enhanced the photocatalytic efficiency of the TiO_2 under optimal operational conditions of 5 ppm of doxycycline, 0.25 g/L of TiO_2, pH 6.5, 120 min, and room temperature. In addition, the changes in morphology, crystal structure, and optical properties of the materials before and after calcination were observed by scanning electron microscopy, X-ray diffraction, and UV-Visible spectroscopy. The reaction kinetics of the doxycycline removal was also investigated based on the Langmuir-Hinshelwood model with a correlation coefficient R^2 of >80%. Results showed that the photocatalytic ability of TiO_2 is stable and enhanced after being calcined at a suitable temperature of 500 °C. This opens up the potential application of TiO_2 in the treatment of emerging organic pollutants in water.

Keywords: TiO_2; Photocatalytic; Doxycycline; Antibiotics; Water treatment

How to Cite: N.T.C. Tien, C.H. Nhut, V.T.T. Thuy, T.T.B. Huyen, L.P.T. Hien, N.N. Huy (2022). Enhancement in Photocatalytic Efficiency of Commercial TiO_2 Nanoparticles by Calcination: A Case of Doxycycline Removal. *Bulletin of Chemical Reaction Engineering & Catalysis*, 17(3), 486-496 (doi: 10.9767/bcrec.17.3.13970.486-496)

Permalink/DOI: https://doi.org/10.9767/bcrec.17.3.13970.486-496

1. Introduction

Titanium dioxide is the most commercially available nanomaterial and has a wide range of applications such as in biology, medicine, science, technology, and the environment. It is easy to come across products containing TiO_2, from products like sunscreen and waterproof tiles to water filters, air conditioners, bio-sensor applications, and drug delivery [1]. The photocatalytic ability is the most prominent feature that has brought TiO_2 to an important nanomaterial in the past 50 years. The commonly used commercial nanoscale TiO_2 material is very popularly known as Degussa P25. In addition to its photochemical properties, TiO_2 has many other advantages such as stability, non-toxicity, chemical stability, availability, and low cost [2]. Although it is not a novel nanomaterial, the multidisciplinary applications of TiO_2 have been discovered more and more.

Besides, the material synthesis method is one of the key ways to bring the outstanding features of TiO_2 into practice with high photocatalytic and economic efficiencies. There have been many reports on the methods of TiO_2 nano-

* Corresponding Author.
Email: nnhuy@hcmut.edu.vn (N.N. Huy);

materials synthesis, such as hydrothermal, sol-gel, solvothermal, sonochemical, direct oxidation, chemical vapor deposition, electrodeposition, and microwave methods [2]. In addition to the synthesis, the modification of TiO_2 nanomaterials has also been proposed, including surface deposition, doping, hybridization, and combining with metals, metal oxides, and non-metals [3]. Based on the synthesis and modification methods, different morphologies of TiO_2 have also been reported. TiO_2 is very diverse in surface morphology in forms of 0D (*e.g.* nanoparticles and nanospheres), 1D (*e.g.* nanorods, nanotubes, and nanowires), 2D (*e.g.* nanosheets and nanoplates), and 3D (*e.g.* hollow spheres, nanoporous, and mesoporous). In environmental remediation, TiO_2 is known as an effective and popular photocatalyst that enhances the decomposition of most organics to inorganic products in the air, water, soil, and sediments, especially emerging organic pollution.

Nowadays, the problem of environmental pollution is becoming more and more serious, especially the emerging organic contaminants (EOCs) with low concentrations, difficult to detect, difficult to decompose, and potentially dangerous to humans and ecosystems. EOCs include several organic or inorganic compounds with complex structural formulas such as by-products of metabolic processes, pesticides, plasticizers, hormones, antimicrobials, surfactants, pharmaceuticals, and personal care products. Among them, the presence of antibiotic residues in the aquatic environment has become a significant concern for the ecological balance and safety of human health globally [4]. In Vietnam, some reports have shown that antibiotic residues appear in surface water and wastewater in some areas [5–8].

Doxycycline (DOX) is a group of broad-spectrum antibiotics belonging to the tetracyclines. It has an antibacterial effect on both gram-negative and positive bacteria. Some reports indicated that DOX occurs in the aquatic environment with residues ranging from 0.11 to 39.5 μg/L at farms in Jiangsu Province, China [9], and <0.05 μg/L in Nigeria [10], 13.62 ng/L in Huangpu River, Shanghai, China [11]. DOX, like some other antibiotics, is stable in the environment and difficult to be biodegraded. The methods to remove DOX in water are mainly adsorption [12,13], photocatalysis [14,15], Fenton processes [16–18], and electrochemical oxidation [19]. Some studies on the synthesis and modification of TiO_2 as photocatalytic materials to remove DOX from water have recently been reported, such as C,S-doped TiO_2 [20], or C-containing TiO_2 [21]. However, the use of commercial TiO_2 material modified by calcination, a simple and economical solution, for photocatalytic removal of DOX has not been published yet.

In this study, the commercial TiO_2 nanoparticle was modified by calcination and employed as a photocatalyst for the removal of DOX in water. The DOX removal was investigated for TiO_2 calcined at temperatures from 200 to 800 °C. The change in morphology, crystal structure, and optical properties of the material was examined by various surface analyses. The effects of operating conditions such as solution pH, material dosage, and DOX concentration on the DOX removal efficiency were investigated and the decomposition kinetics model was also studied.

2. Materials and Methods

2.1 Materials

Degussa P25 TiO_2 nanomaterial was from Merck, Germany with some properties described in Table 1. HNO_3 and NaOH are pure chemicals bought from Xilong, China. Doxycycline (DOX, purity of >99%) was produced by Kunsan Chemical & Pharmaceutical Co., Ltd, China. Double-distilled water used in the test was taken from a water machine in the laboratory.

After calcination, the properties of TiO_2 (*e.g.* P25-500) were analyzed for exploring the changes in morphology and crystal structure through scanning electron microscopy (SEM, JSM-IT200, JEOL, Japan) and X-ray diffraction (XRD, model D2 Phaser, Bruker, Germany), respectively. In addition, the UV-Vis diffuse reflectance spectroscopy (UV-Vis DRS) was used to determine the optical properties and calculate the band gap energy of the TiO_2 nanoparticles using a spectrophotometer (U-4100 Spectrophotometer, Hitachi, Japan). For comparison, titania nanotubes calcined at 500 °C (*i.e.* TNT-500) were also prepared by hydrothermal method and used as referenced photocatalyst [22].

Table 1. Some properties of commercial TiO_2 nanoparticles.

Properties	Unit	Value
BET surface area	m^2/g	52.8
Pore volume	cm^3/g	0.13
Pore diameter	nm	9.6
Particle size	nm	10 – 30
Pore size range	nm	2 – 127

The isoelectric point of the TiO_2 photocatalyst was determined via the titration method [23]. Accordingly, 0.025 g of the material was added to 25 mL of 0.1 M NaCl solution. The initial pH_i was adjusted from 3 to 11 using 0.1 M HCl or 0.1 M NaOH solutions. The mixture was covered and shaken for 48 h, after centrifugation, the final pH of the supernatant was measured (pH_f). In the graph showing the difference between the initial and final pH values ($\Delta pH = pH_f - pH_i$) against the pH_i, the pH value at $\Delta pH = 0$ gives the isoelectric pH value.

2.2 Photocatalytic removal of doxycycline

The photocatalytic experiment on DOX treatment in water using TiO_2 nanomaterials was carried out at room temperature for 120 min. A certain amount of TiO_2 was added to the water with a DOX concentration of 5 ppm. After 30 min of placing the mixture in the dark under magnetically stirring for adsorption-desorption equilibrium, the UVA lamp (365 nm, Panasonic, Japan) was then turned on for photocatalytic reaction. The water sample was then periodically taken and centrifuged at 3000 rpm for 10 min to separate the catalyst particles and the supernatant was then sent for DOX measurement. DOX concentrations before and after treatment were analyzed using a spectrophotometer (DR6000, Hach, USA) at a wavelength of λ = 281 nm.

The removal efficiency of the DOX (H, %) is calculated by the following equation.

$$-\ln\left(\frac{C_t}{C_0}\right) = k_{obs} \times t \quad (1)$$

The pseudo-first-order kinetic equation was used to describe the reaction kinetics of DOX.

$$H\% = \left(1 - \frac{C_t}{C_0}\right) \times 100\% \quad (2)$$

The Langmuir-Hinshelwood model is the most popular model used to describe the kinetics of heterogeneous photocatalysis [24,25], which is written as follows:

$$r = -\frac{dC}{dt} = \frac{k_r \times K_S \times C_0}{1 + K_S \times C_0} = k_{obs} \times t \quad (3)$$

where, r represents the reaction rate, k_r is the apparent reaction rate constant, and K_s (or $K_{L\text{-}H}$) is the equilibrium adsorption constant. C_0 and C_t are the initial concentration and concentration at time t, respectively.

3. Results and Discussion

3.1 Changes in Morphology and Crystalline Structure of TiO_2 Nanoparticles

Figure 1 showed the SEM images of TiO_2 in its commercial form (P25) and after being calcined at 500 °C (P25-500). These TiO_2 nanomaterials had a morphology of particles at the nanoscale, which tends to be clustered togeth-

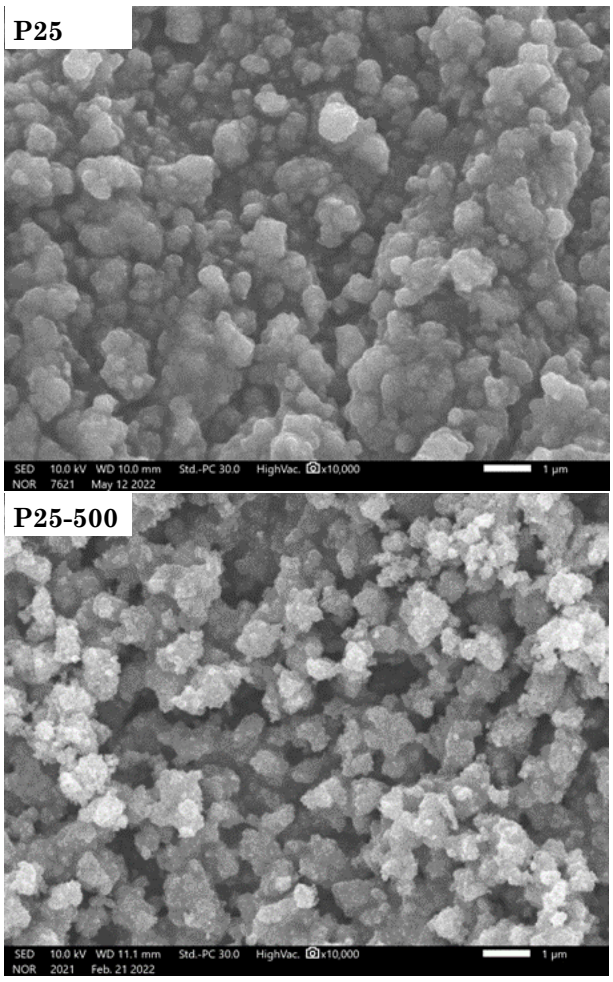

Figure 1. SEM images of commercial P25 and P25 calcined at 500 °C.

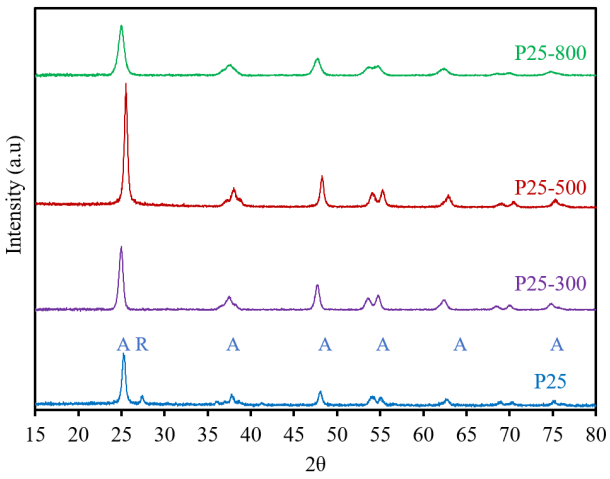

Figure 2. XRD patterns of the pure and calcined P25 TiO_2.

er. The calcination at 500 °C did not significantly change the morphology of the TiO_2 nanoparticles. However, this temperature causes the surface of the particles tending to be fragmented, leading to the rough surface of the grain. Besides, several tiny particles appear on the surface of the large particles, thereby increasing the surface area and pore volume [26,27].

The XRD patterns of P25 before and after calcination are plotted in Figure 2. The P25 TiO_2 nanomaterial exhibits a combined phase of anatase and rutile [22]. The anatase is the main structure due to its higher peak intensities and occupies the majority of XRD patterns at 2θ of 25.24, 37.72, 38.53, 48.00, 54.98, 62.62, 68.92, 69.04, 70.2, and 75.02°, corresponding to the lattice faces of (101), (004), (112), (020), (121), (204), (301), (112), (220), and (215), respectively (JCPDS, card. 21-1272). In addition, the rutile peaks are also observed at 2θ of 27.4 (110), 35.82 (101), and 41.22 (111) (JCPDS, card 21-1276). For the P25 calcined at 500 °C, the characteristic peak of rutile disappeared, while the peak intensity and width of the anatase peaks increased significantly. These results showed a significant improvement in crystallization and growth of the anatase phase after calcination [26]. With a further increase in the calcination temperature, both the height and the sharpness of the anatase peaks tend to decrease. Notably, at 800 °C, the characteristic peaks for the anatase crystalline phase were significantly low and almost disappeared. It demonstrates the destruction of the anatase crystalline structure of TiO_2 at high temperatures.

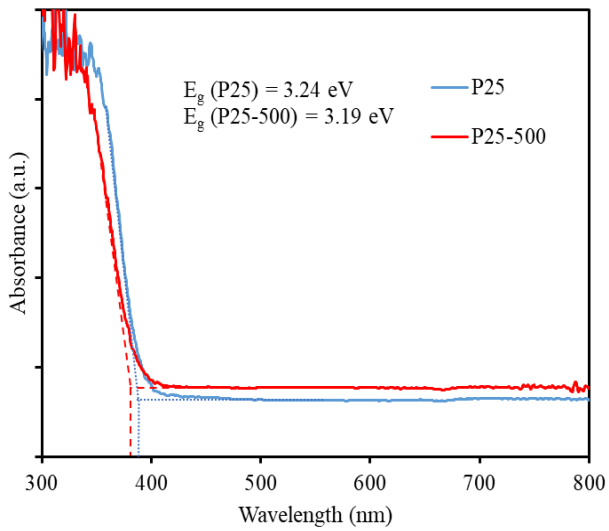

Figure 3. UV-Vis DRS results of P25 and P25-500 materials.

Figure 3 described the results of UV-Vis DRS analysis of P25 and P25-500 materials. Accordingly, P25-500 material has an absorption edge of 383 nm, which was shorter than that of pure P25 (389.1 nm). The bandgap energies of P25 and P25-500 materials were then calculated to be 3.24 and 3.19 eV, respectively. Thus, the calcination process slightly reduced the band gap energy of the P25 material. The reduced bandgap value means that the photon energy level required for an electron to move from the valence band to the conduction band decreases, thus the photocatalytic efficiency could be slightly increased.

3.2 Effect of Calcination on the Photocatalytic Activity

Generally, the calcination temperature of the material significantly affected the structure and material morphology of TiO_2 [22,28,29], thus significantly influencing the photocatalytic removal efficiency. In this study, the effect of calcination on the photocatalytic ability of P25 was investigated in the range of 200–800 °C. The original anatase/rutile ratio of the crystal structure in commercial P25 is about 80:20 [22]. At low calcination temperatures, the crystalline phase component mainly existed in the anatase form since the high activation energy prevents the phase transition of TiO_2 [30]. In some works, the rise of calcination temperature led to the gradual transformation of the anatase to the rutile phase, and the complete change to the rutile form at the calcination temperature of 750 °C [31,32]. As shown in Figure 4, the ability to degrade DOX in water

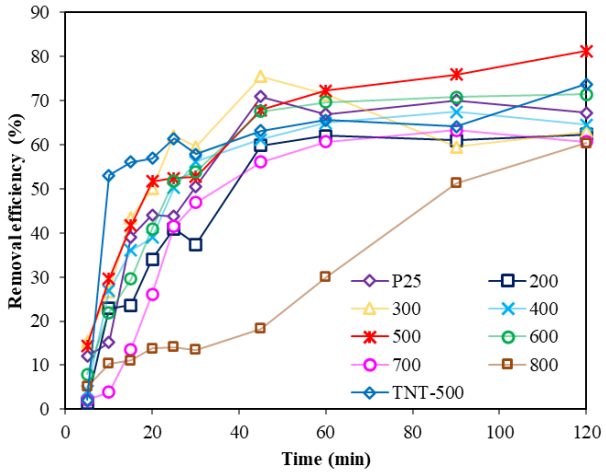

Figure 4. DOX removal by different types of TiO_2 nanomaterial (Conditions: 5 ppm DOX, 0.25 g TiO_2/ L, pH 6.5, UVA irradiation, 120 min).

gradually rose with the increase in the calcination temperature from 200 to 500 °C, but declined from 600 to 800 °C, which could be due to the decrease of anatase crystalline structure, as evidenced in XRD results and reported in the literature [33,34]. This study used the light source from a UVA lamp with the highest intensity at a wavelength of 365 nm. The UV-Vis DRS results of P25-500 show that it has a reduced energy level of the absorbed light to the ultraviolet region, so it may be more efficient in decomposing DOX than P25. The maximum removal efficiency was 81.29% at 500 °C, which was higher than P25 in its original form. When the calcination temperature gradually went up to 800 °C, the removal efficiency rapidly decrease. At high temperatures, there is a growth in crystal size and the agglomeration of particles as well as the low anatase phase. This is not beneficial for photocatalytic activity [32], thus reducing the DOX removal efficiency.

In some works, the combination of both anatase and rutile phases at a certain ratio is the most influential factor in the photocatalytic for TiO_2 [35,36]. However, in this study, it was found that the anatase phase seems to be more effective in photocatalytic DOX removal in water. In fact, Yaemsunthorn *et al.* [37] confirmed that anatase acts as a better oxidant while rutile is a better reducer. Therefore, in this case, P25-500 with its anatase crystalline phase could be more beneficial for DOX removal under UV light irradiation. Besides, P25 calcined at 500 °C and TNT-500 [22] gave stable DOX removal efficiencies, which were better than other TiO_2 types. Previous studies showed that TNTs calcined at 400–500 °C had a higher photocatalytic ability than P25 TiO_2 [26]. In addition, a report by He et al. showed that TiO_2 hollow nanoparticles calcined at 250 °C also have a higher photocatalytic ability than P25 [22,27,28]. However, the photocatalytic ability depends on the target pollutants. In this study, P25 calcined at 500 °C was more suitable to degrade DOX than TNT-500 since it provided better removal efficiency, which is consistent with some other reports [38,39]. Therefore, P25 calcined at 500 °C was chosen as a suitable photocatalyst for further investigation.

3.3 Effects of Operational Conditions on DOX Removal

The effect of initial pH on the DOX removal efficiency is demonstrated in Figure 5(a). The pH value played an important role in photocatalysis since it directly affects the surface charge of the catalytic material and the existing forms of the pollutants in the solution. In this work, the effect of initial pH from 3 to 9 was investigated to determine the role of pH in the photocatalytic removal of DOX in water. In Figure 5(a), when the pH rose from 3 to 6.5, the removal efficiency gradually went up, and then declined with a further increase in pH from 6.5 to 9. The DOX removal efficiency of P25-500 reached the highest value of 81.3% at pH 6.5 (unadjusted pH value).

DOX had three pK_a values of 3.5, 7.07, and 9.13, respectively, corresponding to three existing forms of cationic, zwitterionic, and anionic in acidic, weak to neutral, and alkaline conditions, respectively [17]. Meanwhile, the isoelectric point (pH_{pzc}) of the P25-500 was determined at 6.35 (Figure 5(b)). When the solution pH < pH_{pzc}, the material surface carries a positive charge, whereas DOX carried a negative or neutral charge. The negatively charged DOX exists in the solution at a weakly acidic to neutral medium (pH >4) [14], which explains the increase in removal efficiency when increasing

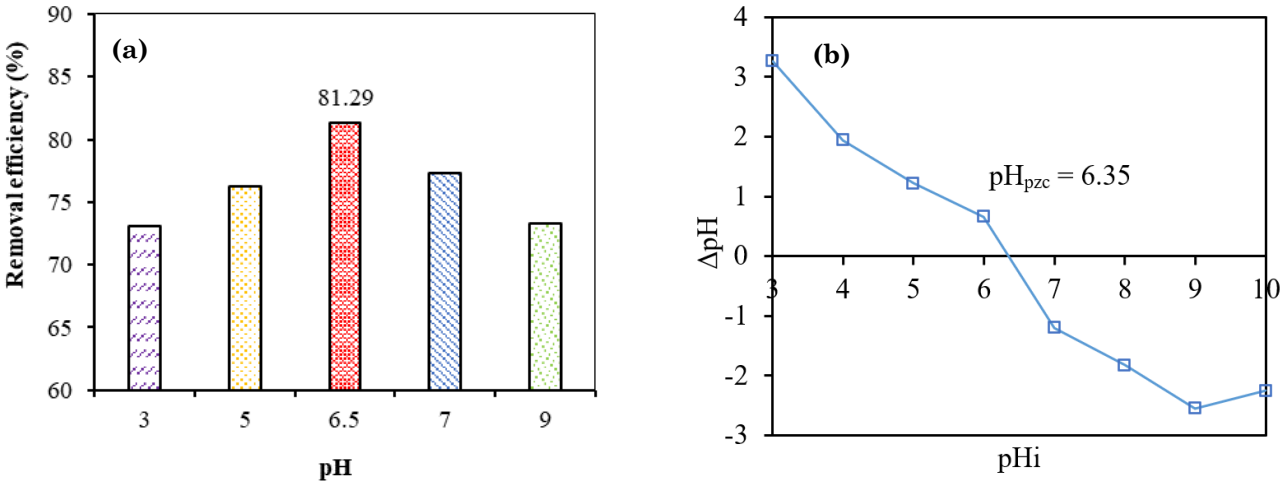

Figure 5. (a) Effect of initial pH on DOX removal and (b) pH_{pzc} of P25-500 material.

the pH from 3 to 6.5. The electrostatic interaction between the material surface and the pollutant is strong for these two opposite charges, thus enhancing the adsorption of DOX on the material surface and leading to an increase in DOX removal efficiency. In contrast, at pH 7, both P25-500 material and DOX exist in negatively charged forms, thus the electrostatic repulsion leads to a decrease in removal efficiency. DOX removal was preferred in the neutral pH range and the unadjusted pH value when DOX was completely dissolved in water. Therefore, in this study, the solution pH was not adjusted for further experiments.

The dosage of material used in the photocatalytic processes should be sufficient for demonstrating a high removal efficiency but not exceed the required dosage for ensuring the economic aspect due to the material cost. Figure 6 depicts the effect of material dosage on the photocatalytic removal of DOX with P25-500 dosage in the range of 0.1–1.0 g/L. With a DOX concentration of 5 ppm, the DOX removal reached the highest removal efficiency at the dosage of 0.25 g/L. Usually, as the amount of material increased, the removal efficiency had the same trend. However, in this case, where the contaminant concentration remained unchanged, larger dosages of the material particles increased the degree of disturbance in the aqueous solution, thus preventing the exposure of the material to the light and reducing the generation of reactive oxygen species (ROS) (*e.g.* hydroxyl radical) during the photocatalysis. Therefore, determining an optimal dosage of materials was one of the essential stages for extending this process for practical applications. In this study, the optimal dosage of P25-500 was determined to be 0.25 g/L.

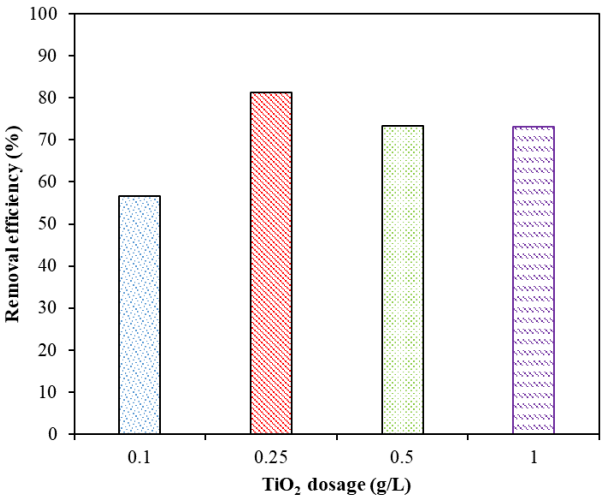

Figure 6. Effect of TiO_2 dosage on DOX treatment efficiency.

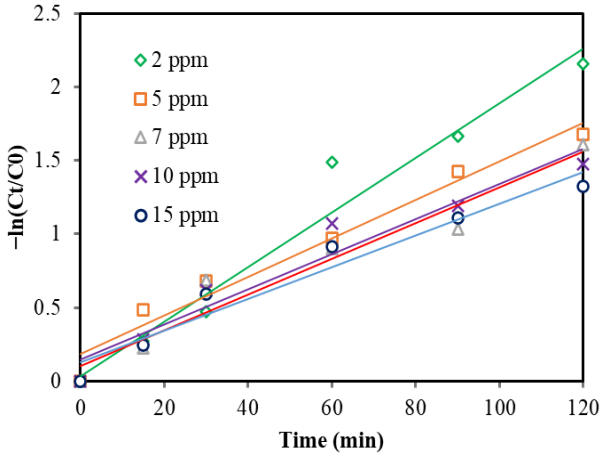

Figure 7. Pseudo-first-order kinetic for different DOX concentrations.

The effect of DOX concentration on photocatalytic removal was carried out with a concentration range of 2–15 ppm. As shown in Figure 7, the removal efficiency decreases with the increase in the pollutant concentration. Under the same operating conditions, high concentrations of DOX required more time and ROS to be degraded and further mineralized. In general, the photocatalytic removal of DOX at different concentrations follows the pseudo-first-order kinetic model with high correlation coefficients of R^2 >0.94 (Table 2). The removal rate

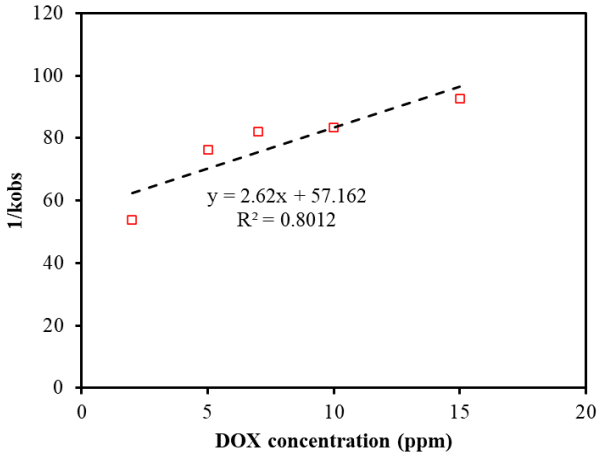

Figure 8. The linear relationship of $1/k_{obs}$ value and initial concentration.

Table 2. Pseudo-first-order kinetic apparent constants of different initial DOX concentrations.

C_0 (ppm)	k_{obs}	R^2
2	0.0186	0.9623
5	0.0131	0.9659
7	0.0122	0.9425
10	0.0120	0.9433
15	0.0108	0.9493

constant was inversely proportional to the DOX concentration.

The Langmuir-Hinshelwood model was one of the models that well describes the heterogeneous photocatalytic process. Figure 8 depicted the suitability of this model for describing the photocatalytic removal of DOX in water using P25-500 material with a correlation coefficient R^2 of 0.8012. Accordingly, the rate constants K_s and K_{L-H} calculated according to the equation are 0.382 mg/(L.min) and 0.046 L/mg, respectively.

3.4 Comparison with Other Studies

There have been many reports related to the synthesis and application of nanomaterials for the photocatalytic removal of DOX. The removal efficiency and reaction rate for each photocatalyst are different since they depend on both the material properties and reaction conditions. Some common materials in this field are ZnO, TiO_2, and Bi_2O_3 (Table 3), where most studies showed the DOX removal efficiency of >80% within 2 h under irradiation. In this study, the use of commercial TiO_2 calcined at 500 °C was able to decompose DOX in water under UVA irradiation and does not require the addition of oxidants. Therefore, it reduces the cost of material synthesis and saves chemicals, equipment, and operating costs, leading to the high feasibility of this study as compared to other reports.

3.5 Proposed DOX Degradation Pathway

During the photocatalytic process, many ROS (*e.g.* hydroxyl radical, singlet oxygen, photo-excited hole, and superoxide) with strong oxidizing properties may play major roles in the degradation of DOX in water. The LC/MS analysis was carried out to determine the fragmentation of DOX during photocatalysis using P25-500 material (Figure 9). Specifically, the DOX molecule is attacked by ROS at the fragile site of $N-(CH_3)_2$, and the opening in the benzene ring forms the intermediate of DOX1 (m/z = 362) [42]. After that, the decomposition of this intermediate forms some products with shorter carbon chains such as DOX2 (m/z = 149) and

Table 3. Photocatalytic decomposition of DOX in the water of some different materials.

Materials	Conditions	Results	Ref.
α-Bi_2O_3/g-C_3N_4	[DOX] = 0.01 g/L [Material] = 0.5 g/L [H_2O_2] = 10 mM Unadjusted pH Xe lamp (150W)	Removal of 79.1% DOX after 30 min	[40]
polymer-ZnO composite	[DOX] = 50 µg/mL [Material] = 0.25 g/L pH = 7 UV-C lamp (30 W)	Removal of 92.7% DOX in 6 h	[14]
C,S-Doped TiO_2	[DOX] = 6.5×10^{-5} M [Material] = 1 g/L 26W Delux UV lamp and 8 W Maxus visible light lamp	Highest removal rate constant: $k_{UV} = 9.0\times10^{-3}$.min^{-1} $k_{Vis} = 7.7\times10^{-3}$.min^{-1}	[20]
MWCNTs/α-Bi_2O_3	[DOX] = 10 mg/L [Material] = 1 g/L 150 W Xe lamp with a UV cut-off filter	Removal of 91% DOX after 120 min	[41]
BiOBr/$FeWO_4$	[Material] = 1 g/L 300 W Xenon lamp	Removal of 90.1% DOX after 60 min	[15]
P25-500	[DOX] = 5 ppm [Material] = 0.25 g/L Unadjusted pH UVA lamp	Removal of 81.29% DOX after 120 min	This study

DOX5 (m/z = 100). These products were then decomposed into simple organic acids such as DOX3 (m/z = 118), DOX6 (m/z = 84), DOX4 (m/z = 102), phenol, ketone, and finally to mineralized products of CO_2 and H_2O [43].

4. Conclusions

In this work, the calcination at 500 °C effectively enhanced the photocatalytic ability of commercial P25 TiO_2 nanoparticles for DOX removal in water. Over 80% DOX at an initial concentration of 5 ppm was removed after 120 min under optimal operating conditions of 0.25 gTiO_2/L, pH 6.5, UVA irradiation, and room temperature. Its removal efficiency was higher than the referenced material of commercial TiO_2 and titania nanotubes. In the reaction, neutral pH was the most effective condition for DOX removal due to the electrostatic attraction of the material surface and the pollutant. The kinetics of DOX decomposition in water by photocatalysis using TiO_2 nanomaterials follows the pseudo-first-order kinetics and Langmuir-Hinshelwood model with high confidence. The k_s and K_{L-H} values calculated by the model are

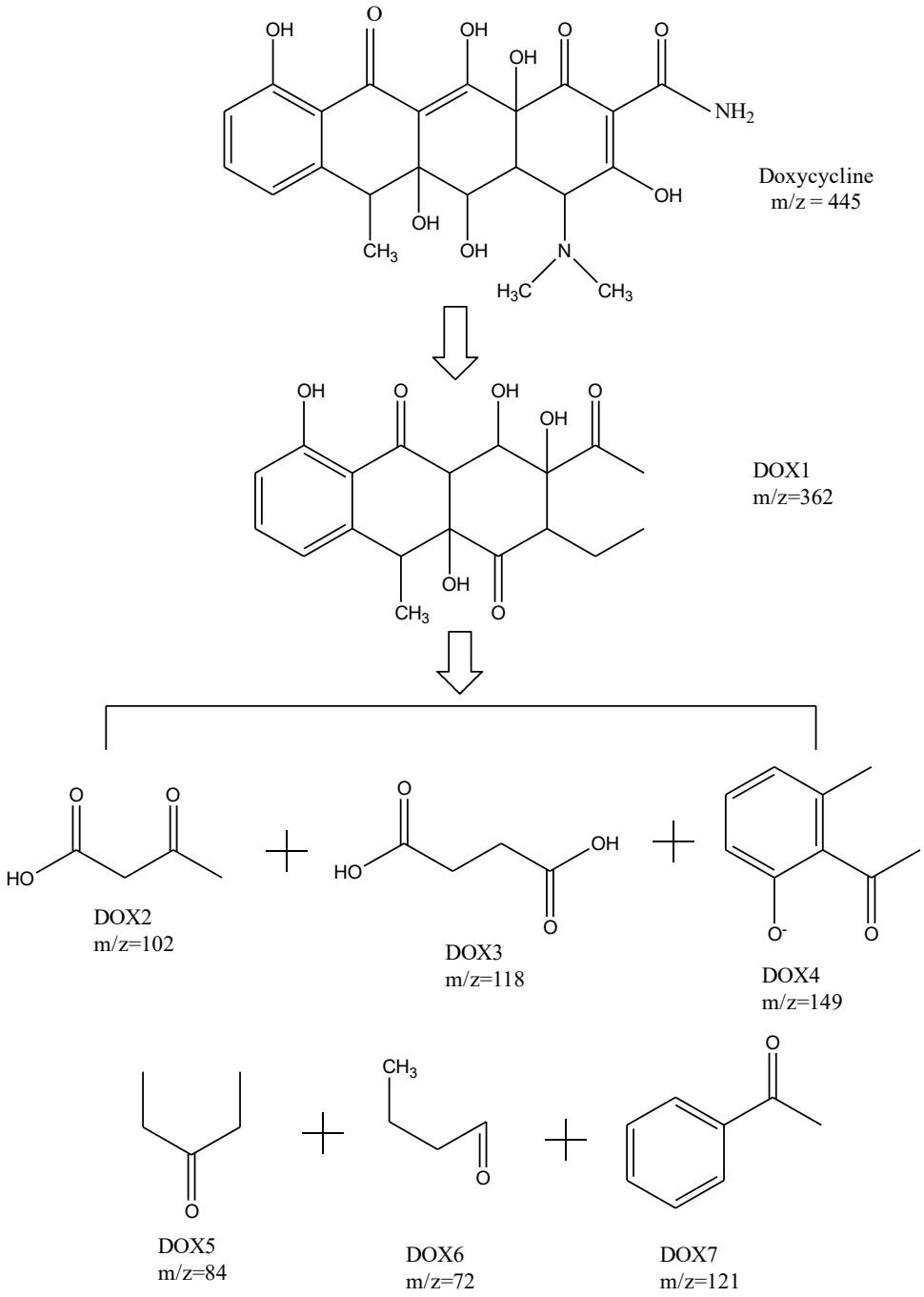

Figure 9. The pathway of DOX degradation during the photocatalysis using P25-500 material.

0.382 mg/(L.min) and 0.046 L/mg, respectively. Future works should focus on evaluating the mineralization and toxicity of the products after the photocatalytic treatment.

Acknowledgement

This research was conducted under the framework of CARE-RESCIF initiative and financially supported by Ho Chi Minh City University of Technology (HCMUT), VNU-HCM under grant number Tc-MTTN-2021-04. We acknowledge the support of time and facilities from Ho Chi Minh City University of Technology (HCMUT), VNU-HCM for this study.

References

[1] Chen, X., Selloni, A. (2014). Introduction: titanium dioxide (TiO_2) nanomaterials. *Chemical Reviews,* 114(19), 9281-9282. DOI: 10.1021/cr500422r

[2] Noman, M.T., Ashraf, M.A., Ali, A. (2019). Synthesis and applications of nano-TiO_2: a review. *Environmental Science and Pollution Research,* 26(4), 3262-3291. DOI: 10.1007/s11356-018-3884-z

[3] Gupta, S.M., Tripathi, M. (2011). A review of TiO_2 nanoparticles. *Chinese Science Bulletin,* 56(16), 1639. DOI: 10.1007/s11434-011-4476-1

[4] Kovalakova, P., Cizmas, L., McDonald, T.J., Marsalek, B., Feng, M., Sharma, V.K. (2020). Occurrence and toxicity of antibiotics in the aquatic environment: A review. *Chemosphere,* 251, 126351. DOI: 10.1016/j.chemosphere.2020.126351

[5] Duong, H.A., Phung, T.V., Nguyen, T.N., Phan Thi, L.-A., Pham, H.V. (2021). Occurrence, distribution, and ecological risk assessment of antibiotics in selected urban lakes of Hanoi, Vietnam. *Journal of Analytical Methods in Chemistry,* 2021, 6631797. DOI: 10.1155/2021/6631797

[6] Rico, A., Phu, T.M., Satapornvanit, K., Min, J., Shahabuddin, A., Henriksson, P.J., Murray, F.J., Little, D.C., Dalsgaard, A., Van den Brink, P.J. (2013). Use of veterinary medicines, feed additives and probiotics in four major internationally traded aquaculture species farmed in Asia. *Aquaculture,* 412, 231-243. DOI: 10.1016/j.aquaculture.2013.07.028

[7] Tran, N.H., Hoang, L., Nghiem, L.D., Nguyen, N.M.H., Ngo, H.H., Guo, W., Trinh, Q.T., Mai, N.H., Chen, H., Nguyen, D.D. (2019). Occurrence and risk assessment of multiple classes of antibiotics in urban canals and lakes in Hanoi, Vietnam. *Science of the Total Environment,* 692, 157-174. DOI: 10.1016/j.scitotenv.2019.07.092

[8] Uchida, K., Konishi, Y., Harada, K., Okihashi, M., Yamaguchi, T., Do, M.H.N., Thi Bui, L., Duc Nguyen, T., Do Nguyen, P., Thi Khong, D. (2016). Monitoring of antibiotic residues in aquatic products in urban and rural areas of Vietnam. *Journal of agricultural food chemistry,* 64(31), 6133-6138. DOI: 10.1021/acs.jafc.6b00091

[9] Wei, R., Ge, F., Huang, S., Chen, M., Wang, R. (2011). Occurrence of veterinary antibiotics in animal wastewater and surface water around farms in Jiangsu Province, China. *Chemosphere,* 82(10), 1408-1414. DOI: 10.1016/j.chemosphere.2010.11.067

[10] Olarinmoye, O., Bakare, A., Ugwumba, O., Hein, A. (2016). Quantification of pharmaceutical residues in wastewater impacted surface waters and sewage sludge from Lagos, Nigeria. *Journal of Environmental Chemistry Ecotoxicology,* 8(3), 14-24. DOI: 10.5897/JECE2015.0364

[11] Jiang, L., Hu, X., Yin, D., Zhang, H., Yu, Z. (2011). Occurrence, distribution and seasonal variation of antibiotics in the Huangpu River, Shanghai, China. *Chemosphere,* 82(6), 822-828. DOI: 10.1016/j.chemosphere.2010.11.028

[12] Aniagor, C.O., Igwegbe, C.A., Ighalo, J.O., Oba, S.N. (2021). Adsorption of doxycycline from aqueous media: a review. *Journal of Molecular Liquids,* 334, 116124. DOI: 10.1016/j.molliq.2021.116124

[13] Abdulsahib, W.K., Ganduh, S.H., Mahdi, M.A., Jasim, L.S. (2020). Adsorptive removal of doxycycline from aqueous solution using graphene oxide/hydrogel composite. *International Journal of Applied Pharmaceutics,* 12(6), 100-106. DOI: 10.22159/ijap.2020v12i6.39118

[14] Mohammadi, A., Pourmoslemi, S. (2018). Enhanced photocatalytic degradation of doxycycline using a magnetic polymer-ZnO composite. *Water Science Technology,* 2017(3), 791-801. DOI: 10.2166/wst.2018.237

[15] Gao, J., Gao, Y., Sui, Z., Dong, Z., Wang, S., Zou, D. (2018). Hydrothermal synthesis of BiOBr/$FeWO_4$ composite photocatalysts and their photocatalytic degradation of doxycycline. *Journal of Alloys Compounds,* 732, 43-51. DOI: 10.1016/j.jallcom.2017.10.092

[16] Borghi, A.A., Silva, M.F., Al Arni, S., Converti, A., Palma, M.S. (2015). Doxycycline degradation by the oxidative Fenton process. *Journal of Chemistry,* 2015. DOI: 10.1155/2015/492030

[17] Bolobajev, J., Trapido, M., Goi, A. (2016). Effect of iron ion on doxycycline photocatalytic and Fenton-based autocatatalytic decomposition. *Chemosphere,* 153, 220-226. DOI: 10.1016/j.chemosphere.2016.03.042

[18] Sierra, R.S.C., Zúñiga-Benítez, H., Peñuela, G.A. (2022). Photo-assisted removal of doxycycline using H_2O_2 and simulated sunlight: Operational parameters optimization and ecotoxicity assessment. *Journal of Photochemistry Photobiology A: Chemistry,* 425, 113697. DOI: 10.1016/j.jphotochem.2021.113697

[19] Miyata, M., Ihara, I., Yoshid, G., Toyod, K., Umetsu, K. (2011). Electrochemical oxidation of tetracycline antibiotics using a Ti/IrO_2 anode for wastewater treatment of animal husbandry. *Water Science Technology,* 63(3), 456-461. DOI: 10.2166/wst.2011.243

[20] Romanovska, N.I., Manoryk, P.A., Selyshchev, O.V., Ermokhina, N.I., Yaremov, P.S., Grebennikov, V.M., Shcherbakov, S.M., Zahn, D.R.T. (2020). Effect of the Modification of TiO_2 with Thiourea on its Photocatalytic Activity in Doxycycline Degradation. *Theoretical and Experimental Chemistry,* 56(3), 183-191. DOI: 10.1007/s11237-020-09650-6

[21] Do, T.C.M.V., Nguyen, D.Q., Nguyen, K.T., Le, P.H. (2019). TiO_2 and Au-TiO_2 Nanomaterials for Rapid Photocatalytic Degradation of Antibiotic Residues in Aquaculture Wastewater. *Materials,* 12(15), 2434. DOI: 10.3390/ma12152434

[22] Nguyen, N.H., Bai, H. (2014). Photocatalytic removal of NO and NO_2 using titania nanotubes synthesized by hydrothermal method. *Journal of Environmental Sciences,* 26(5), 1180-1187. DOI: 10.1016/S1001-0742(13)60544-6

[23] Linh, H.X., Oanh, P.T., Huy, N.N., Van Hao, P., Ngoc Minh, P., Hong, P.N., Van Thanh, D. (2019). Electrochemical mass production of graphene nanosheets for arsenic removal from aqueous solutions. *Materials Letters,* 250, 16-19. DOI: 10.1016/j.matlet.2019.04.115

[24] Du, E., Zhang, Y.X., Zheng, L. (2009). Photocatalytic degradation of dimethyl phthalate in aqueous TiO_2 suspension: a modified Langmuir–Hinshelwood model. *Reaction Kinetics Catalysis Letters,* 97(1), 83-90. DOI: 10.1007/s11144-009-0014-4

[25] Pourmoslemi, S., Mohammadi, A., Kobarfard, F., Amini, M. (2016). Photocatalytic removal of doxycycline from aqueous solution using ZnO nano-particles: a comparison between UV-C and visible light. *Water Science Technology,* 74(7), 1658-1670. DOI: 10.2166/wst.2016.339

[26] Yu, J., Yu, H., Cheng, B., Trapalis, C. (2006). Effects of calcination temperature on the microstructures and photocatalytic activity of titanate nanotubes. *Journal of Molecular Catalysis A: Chemical,* 249(1-2), 135-142. DOI: 10.1016/j.molcata.2006.01.003

[27] He, F., Ma, F., Li, J., Li, T., Li, G. (2014). Effect of calcination temperature on the structural properties and photocatalytic activities of solvothermal synthesized TiO_2 hollow nanoparticles. *Ceramics International,* 40(5), 6441-6446. DOI: 10.1016/j.ceramint.2013.11.094

[28] Vo, T.T.T., Nguyen, H.S., Tran, T.T., Lam, P.T.H., Nguyen, T.T., Nguyen, N.H. (2020). Effects of environmental factors and synthesis conditions on the photocatalytic activity of titanate nanotubes for removal of gaseous formaldehyde. *Research on Chemical Intermediates,* 46(11), 4793-4809. DOI: 10.1007/s11164-020-04247-z

[29] Nguyen, N.H., Khoi, T.T., Hung, T.N., Xuan, Q.V.N., Thi, T.H., Le Thi, P., Thi, T.N. (2021). Photocatalytic disinfection of Coliforms and degradation of natural organic matters in river water using titanate nanotubes. *Environmental Technology*, 43(16), 2553-2567. DOI: 10.1080/09593330.2021.1889039

[30] Mahshid, S., Askari, M., Sasani Ghamsari, M., Afshar, N., Lahuti, S. (2009). Mixed-phase TiO_2 nanoparticles preparation using sol–gel method. *Journal of Alloys and Compounds,* 478(1), 586-589. DOI: 10.1016/j.jallcom.2008.11.094

[31] Shah, A.H., Rather, M.A. (2021). Effect of calcination temperature on the crystallite size, particle size and zeta potential of TiO_2 nanoparticles synthesized via polyol-mediated method. *Materials Today: Proceedings,* 44, 482-488. DOI: 10.1016/j.matpr.2020.10.199

[32] Behnajady, M.A., Eskandarloo, H., Modirshahla, N., Shokri, M. (2011). Investigation of the effect of sol–gel synthesis variables on structural and photocatalytic properties of TiO_2 nanoparticles. *Desalination,* 278(1), 10-17. DOI: 10.1016/j.desal.2011.04.019

[33] Tripathi, A.K., Singh, M.K., Mathpal, M.C., Mishra, S.K., Agarwal, A. (2013). Study of structural transformation in TiO_2 nanoparticles and its optical properties. *Journal of Alloys and Compounds,* 549, 114-120. DOI: 10.1016/j.jallcom.2012.09.012

[34] Horti, N.C., Kamatagi, M.D., Patil, N.R., Nataraj, S.K., Sannaikar, M.S., Inamdar, S.R. (2019). Synthesis and photoluminescence properties of titanium oxide (TiO_2) nanoparticles: Effect of calcination temperature. *Optik,* 194, 163070. DOI: 10.1016/j.ijleo.2019.163070

[35] Scanlon, D.O., Dunnill, C.W., Buckeridge, J., Shevlin, S.A., Logsdail, A.J., Woodley, S.M., Catlow, C.R.A., Powell, M.J., Palgrave, R.G., Parkin, I.P., Watson, G.W., Keal, T.W., Sherwood, P., Walsh, A., Sokol, A.A. (2013). Band alignment of rutile and anatase TiO_2. *Nature Materials,* 12(9), 798-801. DOI: 10.1038/nmat3697

[36] Lv, K., Yu, J., Deng, K., Li, X., Li, M. (2010). Effect of phase structures on the formation rate of hydroxyl radicals on the surface of TiO_2. *Journal of Physics and Chemistry of Solids,* 71(4), 519-522. DOI: 10.1016/j.jpcs.2009.12.026

[37] Yaemsunthorn, K., Kobielusz, M., Macyk, W. (2021). TiO_2 with Tunable Anatase-to-Rutile Nanoparticles Ratios: How Does the Photoactivity Depend on the Phase Composition and the Nature of Photocatalytic Reaction? *ACS Applied Nano Materials,* 4(1), 633-643. DOI: 10.1021/acsanm.0c02932

[38] Hamadanian, M., Reisi-Vanani, A., Majedi, A. (2009). Preparation and characterization of S-doped TiO_2 nanoparticles, effect of calcination temperature and evaluation of photocatalytic activity. *Materials Chemistry and Physics,* 116(2), 376-382. DOI: 10.1016/j.matchemphys.2009.03.039

[39] Lei, X.F., Xue, X.X., Yang, H., Chen, C., Li, X., Niu, M.C., Gao, X.Y., Yang, Y.T. (2015). Effect of calcination temperature on the structure and visible-light photocatalytic activities of (N, S and C) co-doped TiO_2 nano-materials. *Applied Surface Science,* 332, 172-180. DOI: 10.1016/j.apsusc.2015.01.110

[40] Liu, W., Li, Z., Kang, Q., Wen, L. (2021). Efficient photocatalytic degradation of doxycycline by coupling α-Bi_2O_3/g-C_3N_4 composite and H_2O_2 under visible light. *Environmental Research,* 197, 110925. DOI: 10.1016/j.envres.2021.110925

[41] Liu, W., Zhou, J., Zhou, J. (2019). Facile fabrication of multi-walled carbon nanotubes (MWCNTs)/α-Bi_2O_3 nanosheets composite with enhanced photocatalytic activity for doxycycline degradation under visible light irradiation. *Journal of Materials Science,* 54(4), 3294-3308. DOI: 10.1007/s10853-018-3090-x

[42] Yan, X., Qian, J., Pei, X., Zhou, L., Ma, R., Zhang, M., Du, Y., Bai, L. (2021). Enhanced photodegradation of doxycycline (DOX) in the sustainable $NiFe_2O_4$/MWCNTs/BiOI system under UV light irradiation. *Environmental Research,* 199, 111264. DOI: 10.1016/j.envres.2021.111264

[43] Hong, P., Li, Y., He, J., Saeed, A., Zhang, K., Wang, C., Kong, L., Liu, J. (2020). Rapid degradation of aqueous doxycycline by surface $CoFe_2O_4/H_2O_2$ system: behaviors, mechanisms, pathways and DFT calculation. *Applied Surface Science,* 526, 146557. DOI: 10.1016/j.apsusc.2020.146557